TABLE 1 Predictors of Coronary Artery Calcium Progression and Incidence Across Different Definitions

	Continuous Progression Methods				Categorical Progression Methods				Incidence
	Absolute	Log	Square root	Percentage	Hokanson	Raggi	Berry	Risk Categories*	Incidence >0
Age		–	–	–		–			+
Male							+		+
Total cholesterol					+				+
HDL-C		–	–						–
Statin	+	+	+		+	+	+	+	+
SBP		+	+				+	+	+
Hypertension medication	+	+	+		+	+	+	+	
Smoking									
Fasting glucose	+	+	+		+	+	+		
FHCVD									+
BMI									
Baseline CAC	+	–	+	–	+	–		–	NA

"+" = positive independent association with a $p < 0.05$. "–" = inverse independent association with a $p < 0.05$. Empty cells indicate absence of independent association. All models were additionally adjusted for interscan interval. *Risk categories consist of CAC >0 to <10, 10 to <100, 100 to <400, and ≥400 AU.

AU = Agatston unit; BMI = body mass index; CAC = coronary artery calcium; FHCVD = family history of cardiovascular disease; HDL-C = high-density lipoprotein cholesterol; NA = not applicable; SBP = systolic blood pressure.

relative change, particularly in individuals with low baseline scores. Small absolute changes corresponding to large relative differences in those with low baseline CAC are likely to drive classification and result in incongruent associations with CHD risk factors. In addition, the Hokanson and Raggi methods had worse concordance in women than in men. Thus, in men with higher scores, there may be less dependence on specific definitions to categorize CAC progression.

In conclusion, we demonstrate that different CAC progression definitions can result in divergent subject classification in up to 30% of individuals, which may alter research findings or impact individualized clinical decisions. More research is needed to identify which definition most closely associates with CHD outcomes prior to the widespread application of CAC progression as a clinical or research tool.

Andre R.M. Paixao, MD*
Ripa Chakravorty, MD
Amit Khera, MD, MSc
David Leonard, PhD
Laura F. DeFina, MD
Carolyn E. Barlow, MS
Nina B. Radford, MD
Benjamin D. Levine, MD

*Division of Cardiology
University of Texas Southwestern Medical Center
5323 Harry Hines Boulevard
Dallas, Texas 75235-8830
E-mail: andrepaixaobh@gmail.com

http://dx.doi.org/10.1016/j.jcmg.2014.07.019

Please note: This work was supported by grant #NSBRI CA02201 from the National Space Biomedical Research Institute. The authors have reported that they have no relationships relevant to the contents of this paper to disclose.

REFERENCES

1. Budoff MJ, Young R, Lopez VA, et al. Progression of coronary calcium and incident coronary heart disease events: MESA (Multi-Ethnic Study of Atherosclerosis). J Am Coll Cardiol 2013;61:1231–9.

2. Budoff MJ, Hokanson JE, Nasir K, et al. Progression of coronary artery calcium predicts all-cause mortality. J Am Coll Cardiol Img 2010;3:1229–36.

3. McEvoy JW, Blaha MJ, Defilippis AP, et al. Coronary artery calcium progression: an important clinical measurement? A review of published reports. J Am Coll Cardiol 2010;56:1613–22.

4. Berry JD, Liu K, Folsom AR, et al. Prevalence and progression of subclinical atherosclerosis in younger adults with low short-term but high lifetime estimated risk for cardiovascular disease: the Coronary Artery Risk Development in Young Adults study and Multi-Ethnic Study of Atherosclerosis. Circulation 2009;119:382–9.

Value of CMR to Differentiate Cardiac Angiosarcoma From Cardiac Lymphoma

Primary cardiac malignancies are extremely rare (1). The 2 most common tumors (i.e., angiosarcoma and lymphoma) are usually right sided and often located near the right atrial wall and right atrioventricular groove, hampering differentiation on cardiac imaging. We describe the value of cardiac magnetic resonance (CMR) in 12 patients with these tumors (7 angiosarcomas and 5 cardiac lymphomas [all B cell non-Hodgkin, HIV negative], all confirmed by biopsy [n = 11] or autopsy [n = 1]). Patients with

FIGURE 1 Representative Examples of Cardiac Angiosarcoma and Cardiac Lymphoma

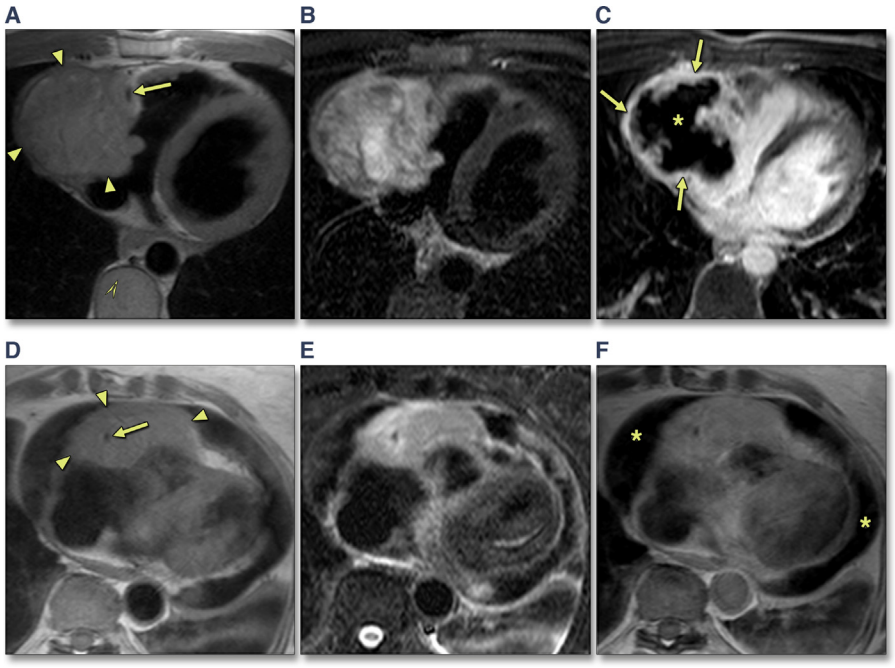

(A to C) Cardiac angiosarcoma. **(D to F)** Cardiac lymphoma. Axial T1-weighted fast-spin-echo cardiac magnetic resonance (CMR) **(A and D)**. Axial T2-weighted short-tau inversion-recovery fast-spin-echo CMR **(B and E)**. Axial late gadolinium enhancement (LGE) CMR **(C)** and T1-weighted fast-spin-echo CMR post-contrast **(F)**. The angiosarcoma presents as a voluminous mass **(A, arrowheads)** arising from the right atrial wall extending to the pericardium, right atrial cavity, and right coronary artery **(A, arrow)** with strong rim enhancement **(C, arrows)** and central liquefaction **(C, asterisk)** on LGE CMR (Online Video 1). The cardiac lymphoma presents as a mass mainly centered in the right atrioventricular groove **(D, arrowheads)**, diffusely surrounding the right coronary artery **(D, arrow)**, extending to the right atrial and right ventricular wall (Online Video 2). Homogeneous enhancement post-contrast administration **(F)**. Also note the presence of a circumferential pericardial effusion **(F, asterisk)**.

angiosarcoma were younger than patients with lymphoma, and dyspnea was the most common complaint at initial presentation for both tumors. Maximal tumor diameter was similar between the tumors (84 ± 22 mm for angiosarcoma vs. 88 ± 19 mm for lymphoma). The right atrial wall was partially to completely invaded by tumor in all patients (**Figure 1A to 1F**, Online Video 1). The right atrial appendage was involved in all patients with an angiosarcoma but in only 1 patient with lymphoma ($p = 0.01$) (Online Video 2). In contrast, all lymphomas diffusely involved the right atrioventricular groove and completely surrounded the right coronary artery (defined as >10 mm tumor tissue around the entire circumference) (**Figures 1D and 1E**). The angiosarcomas showed partial involvement of the right atrioventricular groove in 4 patients and only incompletely (<180°) encased the right coronary artery (RCA) ($p < 0.001$) (**Figure 1A**). Extension toward the right ventricle was present in all lymphomas but only in 3 of 7 angiosarcomas (**Figures 1D and 1E**). The tricuspid valve was involved occasionally and was no different between groups. The CMR images showed a central liquefaction necrosis (or necrotic areas) in 6 of 7 angiosarcomas (i.e., rim enhancement with lack of central enhancement) (**Figure 1C**). This pattern was absent in all lymphomas that showed homogeneous tumor enhancement ($p = 0.015$) (**Figure 1F**). Pericardial effusion was common in both conditions (5 of 7 angiosarcomas [range 10 to 30 mm] and 4 of 5 lymphomas [range 27 to 45 mm]) (**Figures 1D and 1F**). Except in 1 patient with angiosarcoma, enhancement of the pericardial layers was shown on post-contrast CMR images in all patients. Pericardial "nodular" metastasis (including the transverse/oblique sinus) was present about one-half of the time in both conditions, whereas pulmonary metastases were found only in angiosarcomas (3 of 7 patients).

The current results obtained in a small but representative group of patients with cardiac angiosarcoma and HIV-negative lymphoma showed that

JACC: CARDIOVASCULAR IMAGING, VOL. 8, NO. 6, 2015
JUNE 2015:741–9

CMR can help differentiate between these malignant tumors. Tumor location in the right atrial wall and atrial appendage in a younger patient with central necrosis and possibly pulmonary metastasis favors angiosarcoma, whereas lymphomas appear in older patients with diffuse right atrioventricular involvement and RCA encasement and as solid tumors on CMR imaging. Although this is a small sample and features may depend on when the diagnosis was made in the natural history of the disease, it represents a significant number of biopsy-proven tumors with CMR correlation in these rare conditions. CMR may help noninvasive differentiation between angiosarcoma and lymphoma.

Geoffrey C. Colin, MD
Rolf Symons, MD
Steven Dymarkowski, MD, PhD
Bernhard Gerber, MD, PhD
Jan Bogaert, MD, PhD*

*KU Leuven—University of Leuven
Department of Imaging and Pathology
Medical Imaging Research Center
Herestraat 49
B-3000 Leuven
Belgium
E-mail: jan.bogaert@uzleuven.be

http://dx.doi.org/10.1016/j.jcmg.2014.08.011

Please note: Dr. Gerber has received research support from Philips Medical Systems. All other authors have reported that they have no relationships relevant to the contents of this paper to disclose.

REFERENCE

1. Butany J, Nair V, Naseemuddin A, Nair GM, Catton C, Yau T. Cardiac tumours: diagnosis and management. Lancet Oncol 2005;6:219–28.

APPENDIX For accompanying videos and their legends, please see the online version of this article.

Diagnostic Accuracy of Rapid Kilovolt Peak–Switching Dual-Energy CT Coronary Angiography in Patients With a High Calcium Score

Beam-hardening artifacts resulting from heavily calcified plaques in patients with a high coronary calcium score (CCS) may reduce coronary computed tomography angiography (CTA) diagnostic accuracy of the increased false-positive rate (1). A recently introduced computed tomography (CT) technology combines dual-energy computed tomography (DECT) with the latest gemstone detectors, made by a complex rare earth-based oxide that has a chemically replicated garnet crystal structure for gemstone spectral imaging (GSI) integrated into a 64-slice scanner (1). The scanner is equipped with an x-ray source that can switch energy rapidly. The datasets obtained from 2 different energies allow the reconstruction of material decomposed images (MDIs). Two studies demonstrated that coronary CTA using the new DECT offers improvement in terms of image quality compared with standard single-energy CT (1,2). The aim of the present study was to evaluate in patients with a high CCS (>400) the diagnostic accuracy of coronary CTA using DECT with monochromatic images and calcium removal by MDI compared with simulated conventional polychromatic image evaluation as a simulated standard of reference (sSTD) and compare the results with invasive coronary angiography (ICA). We enrolled 75 patients with indication for nonemergent ICA for suspected coronary artery disease (CAD), a CCS higher than 400, and a heart rate of ≤65 beats/min. Coronary CTA was performed with GSI-capable CT (Discovery HDCT 750, GE Healthcare, Milwaukee, Wisconsin) and the followings parameters: 64 × 0.625 mm and gantry rotation time of 0.35 s. Cardiac GSI can simultaneously acquire data by rapidly switching between 80 kVp and 140 kVp energies in <0.252 ms, which produces data that contain minimal misregistration artifacts. The beam was kept at 140 kVp for only a fraction (about one-third) of the radiation time to keep the radiation dose low, whereas during two-thirds of the scan time, the beam was switched to a lower tube current peak (80 kVp). A tube current of ≅600 mA was used. All scans were performed with prospectively electrocardiography-triggered acquisition. First, from the acquired DECT data, conventional polychromatic images that corresponded to a peak tube voltage ranging between standard values of 100 kV and 120 kV were simulated using a 77-keV monochromatic image and used as an sSTD. Second, MDI (iodine minus calcium) derived from the GSI data were used to represent the GSI. The Adaptive Statistical Iterative Reconstruction (ASIR) post-processing algorithm (set at 40%) was used for both types of image reconstruction (sSTD and GSI). The pre-test probability of CAD was intermediate to high (62%). Accordingly, the prevalence of obstructive CAD was 68% (51 of 75 patients). Of patients with ≥50% stenosis, 31 (61%) had multivessel CAD. The mean CCS was 606 ± 253. Eighty percent of patients were pre-treated with intravenous metoprolol before scanning, achieving a mean heart rate of 59 ± 5 beats/min. The mean effective dose was 0.87 mSv for CCS and 3.92 mSv for coronary CTA. The number of coronary segments with excellent image quality was significantly higher with